Melt Rheology of Polypropylene Containing Small Amounts of High-Molecular-Weight Chain. 2. Uniaxial and Biaxial Extensional Flow

M. Sugimoto, Y. Masubuchi, J. Takimoto, and K. Koyama*

Department of Materials Science and Engineering, Yamagata University, 4-3-16 Jonan Yonezawa 992-8510, Japan

Received September 7, 2000; Revised Manuscript Received April 23, 2001

ABSTRACT: Uniaxial extensional flow behavior was measured for the high-melt-strength polypropylene using a Meissner-type rheometer under transient extensional flow with constant tensile strain rate. The equibiaxial extensional flow behavior of the high-melt-strength polypropylene was measured via the lubricated squeezing flow method under constant strain rate. The high-melt-strength polypropylene consists of polypropylene (PP) as a main component and high-molecular-weight polyethylene (PE) component as a long relaxation time component (see part 1). This system is generally believed to be an immiscible system, at least under the quiescent state. Nevertheless, in part 1, we have found that the high-melt-strength PP with very high-molecular-weight PE shows distinctly different shear flow behaviors from conventional PP, e.g., high elasticity and two-step viscosity at low shear rates and strong and weak strain-dependent nonlinear damping functions characterizing fast and slow relaxation processes. In this study, the transient uniaxial viscosity of the high-melt-strength PP melts first increased gradually with time, following the linear viscoelastic rule in which the uniaxial extensional viscosity is 3 times the shear viscosity development. Beyond a certain critical strain, the uniaxial extensional viscosity showed rapid increase, which was referred to as strain hardening. Furthermore, the transient biaxial extensional viscosity showed also the strain hardening behavior over a critical strain. These prominent behaviors are unexpected for conventional PP. The nonlinear upturn behavior was discussed from a high-molecular-weight chain stretching point of view via molecular constitutive equations given by Osaki et al. for bimodal polymer blends.

Introduction

In part 1 of this series of papers, we have examined the linear and nonlinear viscoelastic behavior under shear flow for conventional polypropylene (PP) and high-melt-strength PP. The high-melt-strength PP was synthesized by introducing a small amount of very high-molecular-weight polyethylene (PE) to PP via heterogeneous catalyst, viz. reactor-made binary compositions. The high-melt-strength PP was found to exhibit high elastic response and two-step viscosity at low frequencies (shear rates) and fast and slow relaxation processes in the nonlinear relaxation modulus.

In this paper we further examine uniaxial and biaxial extensional behavior of the high-melt-strength PP. Extensional flow plays an important role in any polymer processing in which the streamlines are not parallel. The presence of nonlinearity in the extensional viscosity is one of the most important characteristics for blow molding, foaming extrusion, thermoforming, film-blowing resins, etc. When stretched or drawn, the strain hardening refers to a melt, which becomes more stiffer and stronger, rather than one that thins and breaks.

The uniaxial extensional viscosity has been extensively studied by many researchers during the past few decades. An extensive collaborate study was carried out on the rheology and processability of three model PEs by IUPAC Working Party.[1,2] The extensional flow of low-density PE (LDPE) and linear low-density PE (LLDPE) have been studied as well. Schlund and Utracki[3] studied on the composition and rheology of various LLDPEs containing three type comonomers polymerized in gas phase and in solution. The extensional behavior is sensitive to the molecular architecture and polymer composition, e.g., the long chain branching such as LDPE [4,5] and high-molecular-weight tails.[6,7]

Only a few publications exist on the biaxial extensional flow behavior of polymer melts in contrast to those on the uniaxial flow,[8−11] though the flow manner is related to many polymer processings. Takahashi et al.[12] reported the biaxial extensional behavior of PS and PP melts utilizing the lubricated squeezing flow method under the constant strain rates. These results exhibit that the strain hardening under biaxial flow is much weaker than that of uniaxial extensional viscosity or disappears even for LDPE with long chain branches.

The sources of the strain hardening have been identified by following three methods: a presence of long chain branching, broad molecular weight distribution, and bimodality of the molecular weight distribution. PP generally has a high-molecular-weight and broad molecular weight distribution but no strain hardening. The main reason why the PP-resin has been difficult to process is recognized as this extensional behavior. One possible method to improve the strain hardening of PP is to give long side branches in postreactor. The modified PP with an electron beam or a peroxide showed the apparent enhancement of the strain hardening.[13,14] This results from constraint of the chain relaxation owing to a presence of long chain branching. Otherwise, introducing "spiky" high-molecular-weight component into a normal molecular mass distribution of a polymer has a possibility to improve the strain hardening.[6,7,15−17]

* To whom correspondence should be addressed. Tel 81-238-26-3058; Fax 81-238-26-3411; e-mail kkoyama@eie.yz.yamagata-u.ac.jp.

10.1021/ma0015525 CCC: $20.00
Published on Web 07/18/2001

Münstedt[6] reported bimodal polystyrene (PS) system with a distinct high-molecular-weight component showed the strong strain hardening. Koyama and Ishizuka[7] carried out research for the effect of a small amount of long relaxation time mode on the strain hardening using the Lodge-type constitutive equation. In recent years the spiky system has been attracting the attention of more and more researchers. Minegishi et al.[16,17] reported that the enhancement of the strain hardening is observed only when the concentration of the spiky high-molecular-weight components reaches and exceeds the critical concentration for molecular entanglement for PS blended with ultrahigh-molecular-weight (uhmw) analogue. The enhancement of the strain hardening is visible only for miscible blends.[3,6,15−17] These results are supported by a computer simulation of Masubuchi et al.[18] by means of a Brownian dynamics simulation for the freely rotated bead−rod model.

The extensional properties of PP has been more and more interesting and important because of its beneficial and desirable physical properties. This study presents the extensional properties of the high-melt-strength PP containing uhmw-PE under uniaxial and biaxial flow. The data obtained are compared to those of the conventional PP. These extensional flow behavior are discussed from the high-molecular-weight chain stretching point of view via molecular constitutive equations given by Osaki et al. for bimodal polymer blends.

Experimental Section

Materials. All the samples were supplied by Chisso Petrochemical Co. (Chiba, Japan). The characteristics of conventional PP (HT1050, PP-A) and the high-melt-strength PP (NEWSTREN/NEWFOAMER: X065HW (PP-B) and X066HW (PP-C)) were described in our previous paper (part 1). PP-B and PP-C were synthesized by a series polymerization of propylene and ethylene employing a heterogeneous catalyst, which generally produce high-molecular-weight and broad molecular weight distribution. The content of uhmw-PE of PP-B and PP-C is 0.4 and 1.0 wt %, respectively.

Rheology Measurements. A. Uniaxial Extension. For uniaxial extensional viscosity measurements, the polymer melts were extruded at a rate of 5 mm/min to sample rods at 230 °C through a die with a single orifice of 2 mm (for PP-B and PP-C) or 3 mm (for PP-A) diameter (Capilograph, Toyoseiki Co. Ltd., Japan). The rods had a diameter of 3−4 mm and the length of 15−20 cm. To eliminate residual stresses of the samples, 15 min of equilibration time was allowed before measurements. Using these rods, uniaxial extensional viscosity at constant strain rates was measured by Meissner-type[19] rheometer at 180 °C. The sample diameter was recorded by a CCD camera and a videotape recorder during the tests in order to confirm the uniform elongation and to calculate the actual strain rates.

B. Biaxial Extension. Biaxial extensional viscosity was measured by a constant area method[8,10] utilizing a lubricated squeezing extensional rheometer (Iwamoto Seisakusyo Co., Ltd., Japan). The geometry is schematically shown in Figure 1. An overview of the method has been reported by Takahashi et al.[12] The main part is composed by parallel plates which diameter is the same with the sample (see Figure 1). The upper plate is computer-controlled to drive at an exponentially decreasing speed so as to realize the constant strain rate. At the center of the lower plate a pin was fixed to prevent the lubricated sample from sliding out of the center of the jig. The upper plate has a hole to accommodate the pin. For the biaxial extensional measurements the samples were prepared by compression molding at 230 °C into the disk shape of 20 mm diameter and 5 mm gap height. A hole of 1.5 mm diameter was drilled at the center of the sample to accommodate a pin fixed on the lower disk. To achieve a uniform deformation, we used silicone oils with kinematic viscosities ranging from a minimum of 5×10^3 to a maximum of 1×10^6 cSt (at 25 °C) as a lubricants. The silicone oils were applied to the upper and lower plates and the sample.

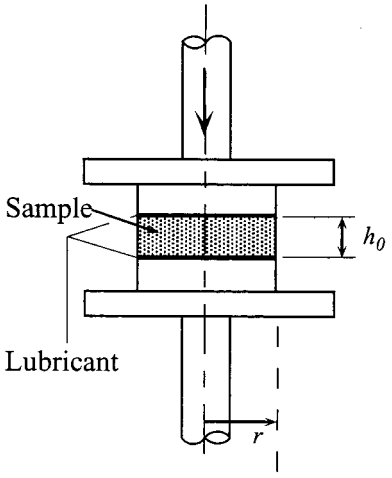

Figure 1. Schematic diagram of lubricated squeezing geometry for biaxial extensional measurement.

The biaxial extensional strain ϵ_B is given by the following equation, assuming a uniform and ideal deformation for incompressible materials:

$$\epsilon_B = -\frac{1}{2}\ln\left\{\frac{h(t_1)}{h(0)}\right\} \tag{1}$$

where $h(0)$ and $h(t_1)$ are the sample thicknesses at the extensional time $t = 0$ and t_1, respectively. The strain rate $\dot{\epsilon}_B$ is given by

$$\dot{\epsilon}_B = \frac{d\epsilon_B(t)}{dt} \tag{2}$$

The net stretching stress $\sigma_B(t)$ is defined from the thrust force $F(t)$, neglecting the surface tension and inertia force:

$$\sigma_B(t) \equiv \frac{F(t)}{\pi r^2} \tag{3}$$

where r is a plate diameter. Thus, the biaxial extensional viscosity $\eta_B^+(t,\dot{\epsilon}_B)$ is given by the following equation:

$$\eta_B^+(t,\dot{\epsilon}_B) = \sigma_B(t)/\dot{\epsilon}_B \tag{4}$$

The biaxial extensional measurements were done at 180 °C. To eliminate residual stresses of the samples, each test was carried out after 15 min of equilibration time at the measurement temperature.

The biaxial extensional viscosity is affected by the viscosity of the lubricant.[11,12,20,21] Papanastasiou et al.[20] and Nishioka et al.[21] reported the effect of the oil viscosity; too much low viscosity results in rapid lubricant squeezing out, and too much high viscosity gives rise to shear deformation of the sample. We used the silicone oil with viscosity of 5×10^4 cSt (at 25 °C) which attained ideal deformation and gave no extra influence on the biaxial extensional stress for each samples.

Results

Uniaxial Extensional Flow Behavior. Figures 2−4 illustrate $\eta_B^+(t, \dot{\epsilon}_B)$ for various $\dot{\epsilon}_E$ at 180 °C for PP-A, -B, and -C, respectively. The solid lines in the figure are the 3-fold linear viscosities $3\eta^+(t)$. The extensional viscosities of PP-A increased smoothly for various extensional strain rates. There was no upward deviation

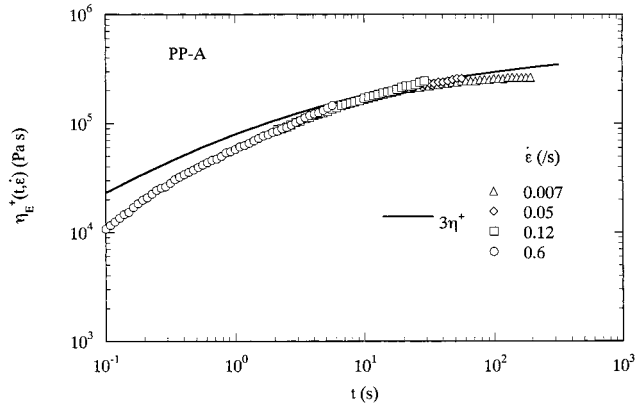

Figure 2. Variation of transient uniaxial extensional viscosity with time at constant strain rates and temperature of 180 °C for PP-A. The solid line indicates 3 times the dynamic viscosity, $3\eta^+$ (see part 1), at 180 °C.

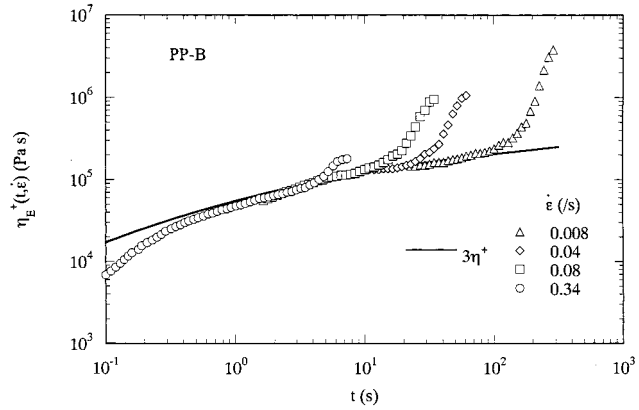

Figure 3. Variation of transient uniaxial extensional viscosity with time at constant strain rates and temperature of 180 °C for PP-B. The solid line indicates 3 times the dynamic viscosity, $3\eta^+$ (see part 1), at 180 °C.

from the linear viscosity within the strain rate measured, $\eta_E^+(t)$ was independent of the strain rates. $\eta_E^+(t)$ of PP-A had a tendency to follow the linear viscoelasticity rule:[22] $\eta_E^+(t) = 3\eta^+(t)$ in the limit of steady state ($t \rightarrow \infty$). Likewise, η_E^+ for PP-B and -C increased smoothly with time within small strains. These samples which contain a small amount of PE with high molecular weight, however, exhibited remarkable upward deviations in η_E^+ called "strain hardening", depending on the extensional strains. This is unexpected behavior for conventional linear PP as mentioned before.

Equibiaxial Extension Flow Behavior. Figure 5 shows the transient biaxial extensional viscosity $\eta_B^+(t,\dot{\epsilon}_B)$ of PP-A for various strain rates at 180 °C. The solid line represents $6\eta^+(t)$, where $\eta^+(t)$ is the shear viscosities within the linear viscoelastic region. For PP-A $\eta_B^+(t,\dot{\epsilon}_B)$ at the low strain rate which section accorded with that at the high strain rate was nearly equal to 6 times $\eta^+(t)$, as should be expected from linear viscoelastic rule. This behavior is similar to that in uniaxial extensional flow. After the smooth increase in early stage, the transient viscosity $\eta_B^+(t)$ appears to be steady during about 0.6−0.9 of the Hencky strain. In the final stage η_B^+ returned to the level of $6\eta^+$. The strain hardening which η_B^+ deviated from the linear viscosity was not observed.

Figures 6 and 7 show the transient viscosities of PP-B and -C, respectively. In the early stage the transient viscosities of the samples increased smoothly with time. η_B^+ tends to follow the linear viscoelastic rule independent of three strain rates ϵ_B. Over a certain critical strain, however, PP-B and -C showed a deviation from the linear viscoelastic region. This strain hardening is especially noteworthy in the case of biaxial extensional flow, since the strain hardening under biaxial flow is generally much weaker than that under uniaxial extensional flow or disappears.[23−25] The reproducibility of the strain hardening at the lower strain rates was carefully inspected by utilizing silicone oils with various

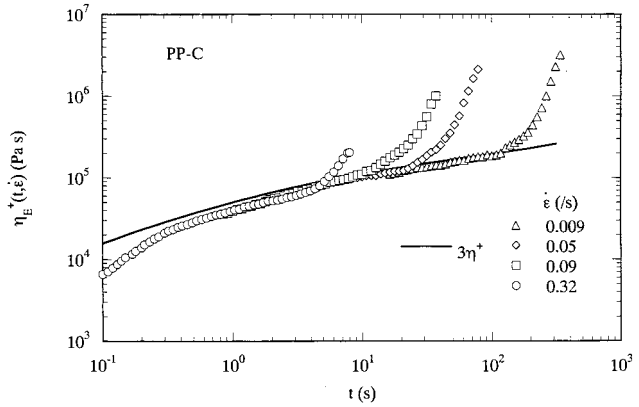

Figure 4. Variation of transient uniaxial extensional viscosity with time at constant strain rates and temperature of 180 °C for PP-C. The solid line indicates 3 times the dynamic viscosity, $3\eta^+$ (see part 1), at 180 °C.

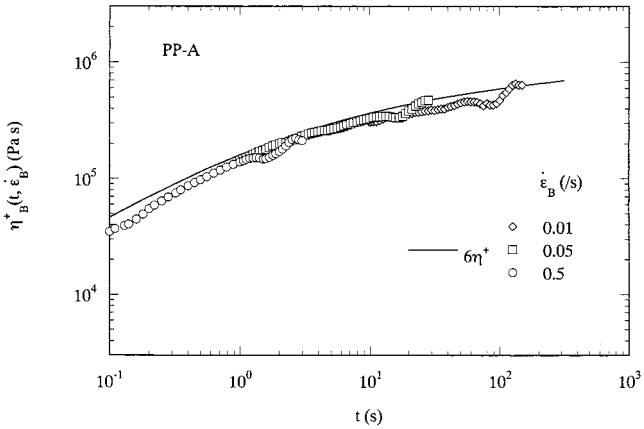

Figure 5. Variation of transient biaxial extensional viscosity with time at constant strain rates and temperature of 180 °C for PP-A. The solid line indicates 6 times the dynamic viscosity, $6\eta^+$, at 180 °C.

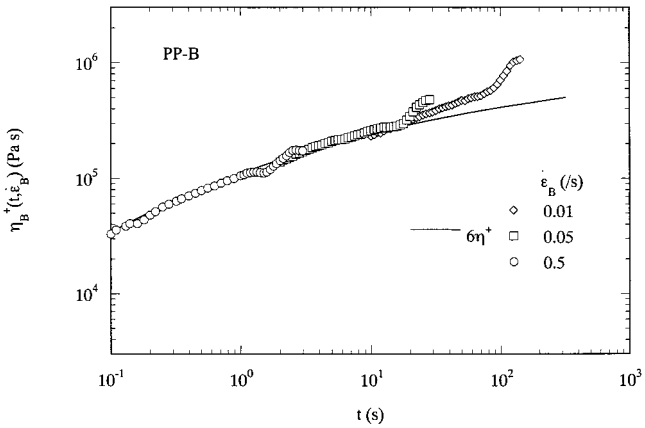

Figure 6. Variation of transient biaxial extensional viscosity with time at constant strain rates and temperature of 180 °C for PP-B. The solid line indicates 6 times the dynamic viscosity, $6\eta^+$, at 180 °C.

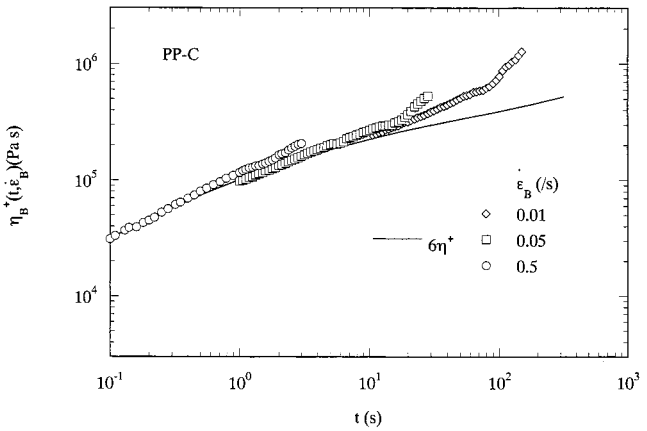

Figure 7. Variation of transient biaxial extensional viscosity with time at constant strain rates and temperature of 180 °C for PP-C. The solid line indicates 6 times the dynamic viscosity, $6\eta^+$, at 180 °C.

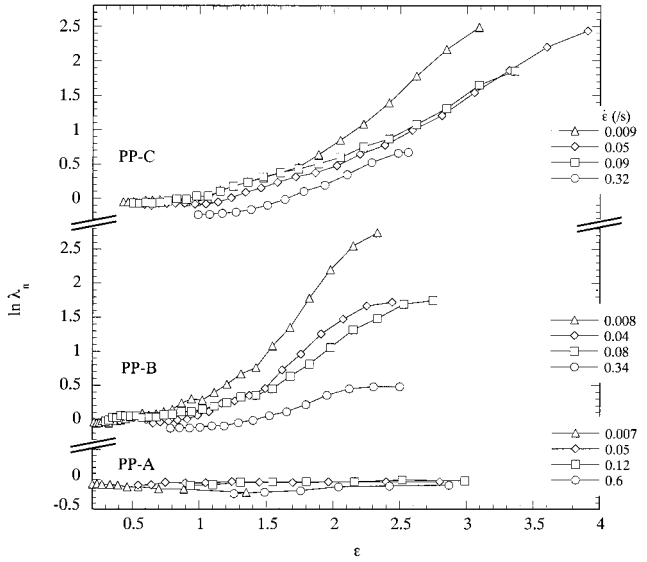

Figure 8. Nonlinear parameter as a function of strain for uniaxial extensional flow of PP-A, PP-B, and PP-C at 180 °C. The strain rates are indicated in the figure.

viscosities. This cannot be related to the effects of lubricant loss or of the viscosity of the silicone oil.

Discussion

Uniaxial Extensional Flow. The magnitude of the strain hardening, nonlinearity parameter λ_n, can be defined by[14,26,27]

$$\lambda_n \equiv \frac{\eta_E^+(t,\dot{\epsilon})}{3\eta^+(t)} \tag{5}$$

where λ_n is the nonlinear viscoelastic element of the extensional flow and $3\eta^+(t)$ is the 3-fold linear viscosity. Figure 8 shows a logarithmic plot of λ_n against ϵ. The strain hardening behavior of PP-B and PP-C can be clearly seen. The critical strain for rupture of the strand was improved according to a concentration of PE (0.4 → 1 wt %). Otherwise, what has to be noticed is the dependence of the nonlinear parameter on strain rates: the stronger the strain hardening, the lower the strain rate. We will return to this point later.

Biaxial Extensional Flow. The steady-like η_B was observed for PP-A (see Figure 5). Ebrahimi et al.[25]

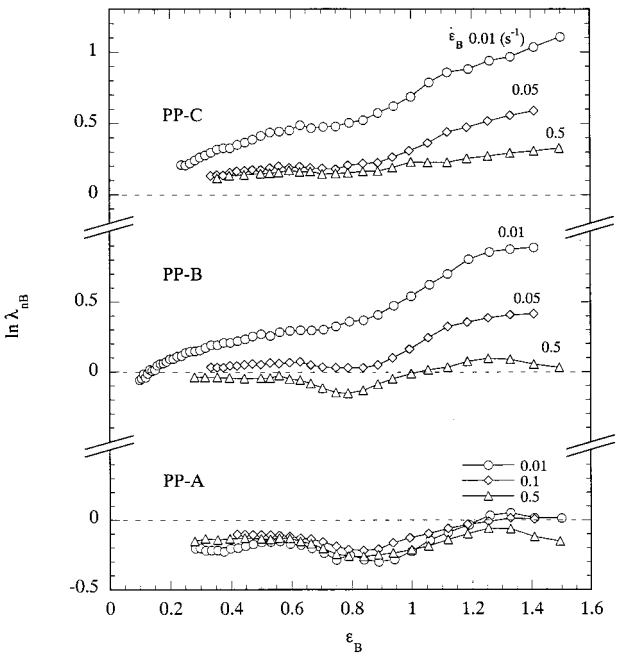

Figure 9. Nonlinear parameter as a function of strain for biaxial extensional flow of PP-A, PP-B, and PP-C at 180 °C. The strain rates are indicated in the figure.

reported a quasi-steady state where η_B decreases with increasing strain for anionic PS. In our case, PP-A has a broad molecular weight distribution; it would need further consideration whether the η_B behavior of PP-A is the quasi-steady state.

In the same manner with eq 5, the nonlinearity parameter for biaxial extension λ_{nB} is defined by

$$\lambda_{nB} \equiv \frac{\eta_B^+(t,\dot{\epsilon}_B)}{6\eta^+(t)} \tag{6}$$

Figure 9 shows a logarithmic plot of λ_{nB} against ϵ_B. When comparing Figure 9 with Figure 8, it is evident that the strain hardening is less intensive under the biaxial extension than the uniaxial extension. This behavior is observed by Meissner et al.[23,28] and Takahashi et al.[12,29] The different flow behavior suggests differences in the chain stretching manner under uniaxial and biaxial extensional flows.

Morphology of Extended Strand. Our previous result on the TEM micrograph (see part 1) indicated the domain structure, assigned to high-molecular-weight PE. To examine the effect of deformation of the domains on extensional behavior, we rapidly cooled the samples in ice/water, immediately after the Hencky strain became 1.2 at the strain rate of 0.1 s^{-1}. To suppress the relaxation of the rod, the extended rod was hold by a clip and then cut. To observe the morphologies, the trimmed sample embedded in epoxy resin was stained by RuO_4 vapor for 12 h at room temperature. Then the sample was sectioned using an ultramicrotome with a diamond knife. Figure 10a,b represents the morphologies before and after the elongation in the center of the rod. The vertical direction of Figure 10 is the extensional direction. For PP, lath- and crosshatched lamellar arrangements are usually observed.[30,31] The morphology are not clear in our case. This ambiguous lamellar structure of PP (light region) may be due to the low crystallization temperature. It is reported that PP quenched from melt into dry ice/ethanol has unclear

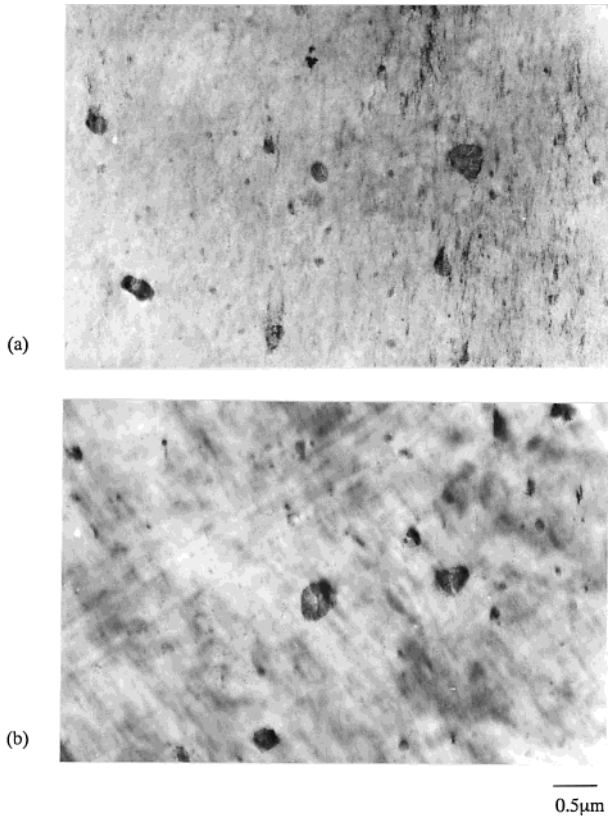

Figure 10. TEM micrographs of PP-H1 strands (a) before and (b) after elongation at 180 °C. The Hencky strain is 1.2 and the strain rate is 0.1 /s. The vertical direction is the extensional direction.

morphology owing to its nodule-like domains as a result of clustering of microcrystals which could not grow into sheet crystals.[32] The dark region is assigned to the PE phase, in which much thicker lamellar crystals characteristic of PE than those of PP can be observed. Sano et al.[32] reported the structural changes of PP and HDPE during RuO_4 staining by monitoring change of peak intensities of carboxylic acid, carboxylate, and ruthenium oxide before and after staining in infrared spectra. For PE, the results showed oxidation and formed carbonyl groups colored the polymer. As regards to PP, the oxidation behavior was almost the same as that for PE, but the saturated amount of carbonyl groups was smaller, corresponding to the lower degree of staining. This provides difference of the image contrast between PP and PE.

Figure 10 shows that the PE domains still keep the shape even after large deformation, at which the strain hardening property emerges. The viscosity ratio of the domains to the major components is large enough, so that those would behave as rigid particles owing to the extremely high molecular weight as mentioned later.

Influence of Strain Rate on the Strain Hardening. From Figure 8 and Figure 9 a fascinating indication may be drawn concerning the effect of extension rates on strain hardening behavior. The more pronounced strain hardening was observed at the lower strain rate under both the uniaxial and biaxial extensional flows. For example, for PP-B at 0.5 s^{-1}, a deviation from the linear viscoelastic region is not apparent, though strong strain hardening could be seen at lower strain rates. According to the Doi and Edwards theory,[33] the high extension rates prevent a primitive chain from the contraction, so that it causes contour length stretching above an equilibrium length. Thus, the higher extensional rates can be related to the more intensive strain hardening under extensional flow, while at enough low strain rates a chain retracts quickly and the tube length does not change. In fact, this behavior has been observed for many polymeric materials, e.g., PS, HDPE, LDPE, etc. On the other hand, some exceptions do exist for the modified PP[14,27] and LLDPE.[3,34] Hingmann and Marczinke[27] reported the marked strain hardening at lower strain rates but weakness at higher strain rates for modified PP via cross-linking agents. They suggested that this might be due to a very small amount of long chain branches (less than 3 per molecule) and a variety of different molecular structures. A similar behavior is reported by Kurzbeck et al.[14] for electron beam irradiated PP. Münstedt and Kurzbeck[34] reported that a significant strain hardening did not occur at higher strain rates (>1 s^{-1}) for LLDPE, which is a mixture of two metallocene-type copolymer. They postulated that the extensional behavior resulted from the immiscibility of the high-molecular-weight linear chains with short chains branching. In our case the behavior is, however, not responsible for the long or short chain branching. One possible explanation could be due to the inhomogeneity of PP-B and PP-C which were composed of PP and PE. TEM micrographs (see Figure 10) indicated the undeformable domain structure, ca. 0.1−0.4 μm in a diameter. The effect of rigid particles on the rheological properties has been reported by several authors.[35−38] The strain hardening property becomes weaker or disappears by an addition of rigid particles. For acrylonitrile−butadiene−styrene copolymer (ABS) melts, Takahashi et al.[39] reported that the hard particles (ca. 0.1−0.5 μm in a diameter) distinctly make the strain hardening property weakened, leading to disappearance at a butadiene content of over 20 wt % at all the strain rates tested. It may be that the rigid domains including in PP-B and PP-C affect the dependence of strain hardening on the extensional strain rates. However, some rheological behaviors of PP-B and PP-C cannot be explained merely by the influence of domains. As we discussed carefully in part 1, we consider that the unusual behaviors of PP-B and PP-C may result from a part of "effective" uhmw-PE chains dissolved into PP. Viewed in this light, the description above may give rise to an assumption of the two competing factors: increasing the transient viscosity owing to the effective high-molecular-weight PE, on one hand, and reducing it because of the presence of the rigid domains, on the other. However, even if assuming a presence of the domain structure in the melts, the content of the particles is much fewer than the case such as ABS copolymer mentioned before.

Another possible explanation could be the effect of constraint release by fast flow. Recently, Marrucci[40] and Marrucci and Ianniruberto[41] advanced an important theory on convective constraint release (CCR) which should play a significant role in the nonlinear range. They have pointed out that fast flows convect away the polymer molecules constraining a given chain and thus destroy the tube surrounding that chain faster than the reptation out of the tube. In such cases, it is likely that the predominant relaxation mechanism is not reptation but the convective constraint release. From this viewpoint one may say as given below. The small extension rate $\dot{\epsilon}$ ($\dot{\epsilon}_B$) examined here is already longer than reciprocal of the characteristic relaxation time τ_R^{-1} concerning

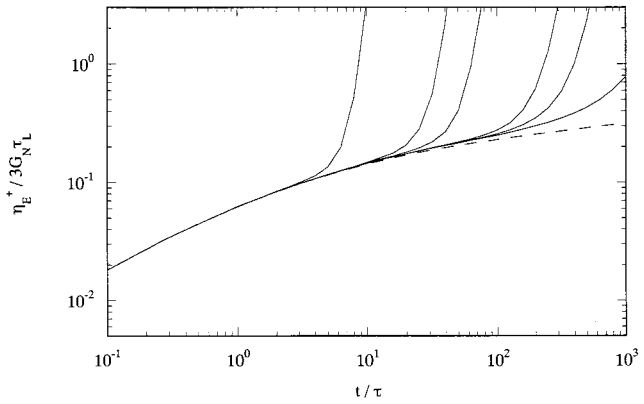

Figure 11. Reduced uniaxial extensional viscosity of a bimodal polymer with H-component ($\phi_H = 1$ wt %) as a function of time at various reduced rates of extension: 0.5, 0.1, 0.05, 0.01, and 0.005 from left to right. The broken line depicts the contribution of the L-component.

the extension of the longer chain (PE) because of its huge molecular weight. With increasing the $\dot{\epsilon}$ ($\dot{\epsilon}_B$) the relaxation of the longer chain was promoted by CCR; shorter chain (PP) was convected away out of a constrained chain.

Estimation of the High-Molecular-Weight Chain Stretching. As the data in Figures 3, 4, 6, and 7 illustrated, PP-B and -C have a large strain hardening. The distinct strain hardening of the PP-B and -C suggest entanglement of PE with high molecular mass. Enhancement of the strain hardening via the high-molecular-weight chain is valid only for the miscible system. PP and PE are generally believed to be an immiscible system, at least under the quiescent state. The results (in part 1 and this study), however, implied the presence of dissolved PE chains into PP and phase-separated PE (domains). It is reported that the phase dissolution is induced by high shear flow field in an injection machine even for PP and PE.[42] However, PP-B and PP-C did not undergo such high shear flow. The unusual flow behavior cannot be attained by a simple mixing via an extruder. One possible explanation could be that high-molecular-mass PE dispersed finely within PP during the polymerization process.

The average molecular weight of PE introduced into PP is not definite, but it is clear that the PE has higher molecular weight and thus much higher relaxation mode than those of PP. The intrinsic viscosity [η] in tetralin at 135 °C of the high-molecular-weight PE (solo polymerization of ethylene without no polymerization of propylene) was 26 dL/g. Extrapolation of the relationship between [η] and the weight-average molecular weight $\bar{M}_w$[43] gave $\bar{M}_w \approx (4-5) \times 10^6$. [$\eta$] and $\bar{M}_w$ of whole polymer (PP-B and PP-C) are 3.0 dL/g and $\bar{M}_w = 5 \times 10^5$, respectively. In part 1, the bimodal molecular weight distribution could be clearly seen for some fractionated sample, though there were not two peaks for the whole polymer. Here, for extensional flow, we attempt to estimate the role of a small amount of higher molecular weight chain that is dissolved into lower molecular weight polymer.

Osaki et al.[44] reported an estimation on the nonlinear flow properties (two-step stress overshoot in shear flow and strain hardening in uniaxial flow) for binary polymer blends (PS and its high-molecular-weight analogue). The extensional stress caused by the high-molecular-weight chain (H-chain) was calculated via a simple dumbbell model. They utilized constitutive equations proposed for the comb-shaped branch polymer by McLeish and Larson[45] to estimate the chain orientation and stretching independently. We shall show an example calculating the extensional stress growth function of the binary system containing small amounts of uhmw-components by this method, assuming that all the H-chain (high-molecular-weight PE) can dissolve into the low molecular mass chain (L-chain, viz. PP) matrix and the H-chain can entangle each other within the L-chain.

Assuming a characteristic time for the orientation as the maximum relaxation time, the orientation tensor **S** of the end-to-end vector **r** obeys following equations:

$$\frac{\partial \mathbf{rr}}{\partial t} = \mathbf{K}\cdot\mathbf{rr} + \mathbf{rr}\cdot\mathbf{K}^T - \frac{1}{\tau_H}\left(\mathbf{rr} - \frac{1}{3}\mathbf{I}\right) \tag{7a}$$

$$\mathbf{S} = \frac{\mathbf{rr}}{tr\mathbf{rr}} \tag{7b}$$

$$\mathbf{K} = \frac{1}{2}\begin{bmatrix} 2\dot{\epsilon} & 0 & 0 \\ 0 & -\dot{\epsilon} & 0 \\ 0 & 0 & -\dot{\epsilon} \end{bmatrix} \tag{7c}$$

where **K** is the deformation rate tensor, **I** is the unit tensor, τ_H is the maximum relaxation time of H-chain, and **S** is the orientation tensor. The time evolution of the stretch ratio of the H-chain is given by a characteristic time for the chain stretching τ_R as

$$\frac{\partial \lambda}{\partial t} = \lambda \mathbf{K}:\mathbf{S} - \frac{1}{\tau_R}(\lambda - 1) \tag{8}$$

Finally, a contribution of the H-chain to stress is expressed as

$$\sigma_H = 3G_N\phi_H{}^2\lambda^2\mathbf{S} \tag{9}$$

Here ϕ_H is the concentration of the H-components, and G_N is the plateau modulus.

When the molecular weight of H-chain is much larger than that of L-chain, eqs 8 and 9 lead to respectively

$$\frac{\partial \mathbf{rr}}{\partial t} = \mathbf{K}\cdot\mathbf{rr} + \mathbf{rr}\cdot\mathbf{K}^T \tag{10}$$

$$\frac{\partial \lambda}{\partial t} = \lambda \mathbf{K}:\mathbf{S} \tag{11}$$

We used eqs 10 and 11 for the estimation of σ_H under an assumption of $\dot{\epsilon}\tau_H \gg \dot{\epsilon}\tau_R \gg 1$. We utilized the stress growth function data of PP-A as that of the L-chain. The plateau modulus of the L-chain (PP) is 4.27×10^5 Pa.[46]

The result for the case of $\phi_H = 0.01$ is shown in Figure 11 as an example. The reduced viscosity growth function, $\eta^+/G_N\tau_L$, is plotted against reduced time, t/τ_L, at various reduced extensional rates, $\dot{\epsilon}\tau_L$. It indicates the strong strain hardening regardless of a very small amount of H-chain at each strain rate, where the L-chain does not exhibit any nonlinear features.

Figure 12 shows the reduced stress growth, σ/G_N, against the Hencky strain for the polymer with a bimodal molecular weight distribution obtained from Figure 11. In Figure 12, the reduced stress increases with strain. Over an extensional strain, the reduced stresses at various rates converged on a single value,

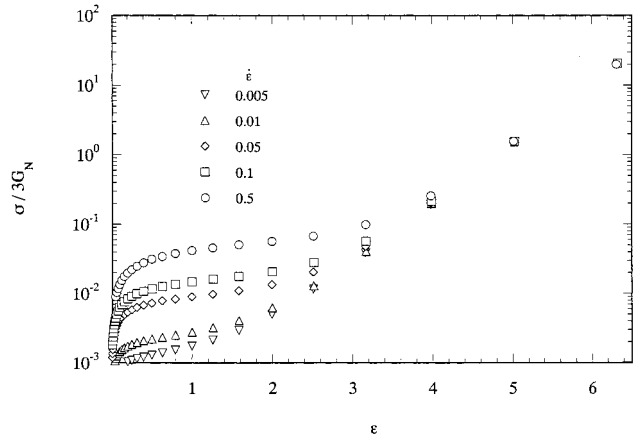

Figure 12. Reduced stress growth obtained from Figure 11 as a function of Hencky strain at various reduced rates of extension.

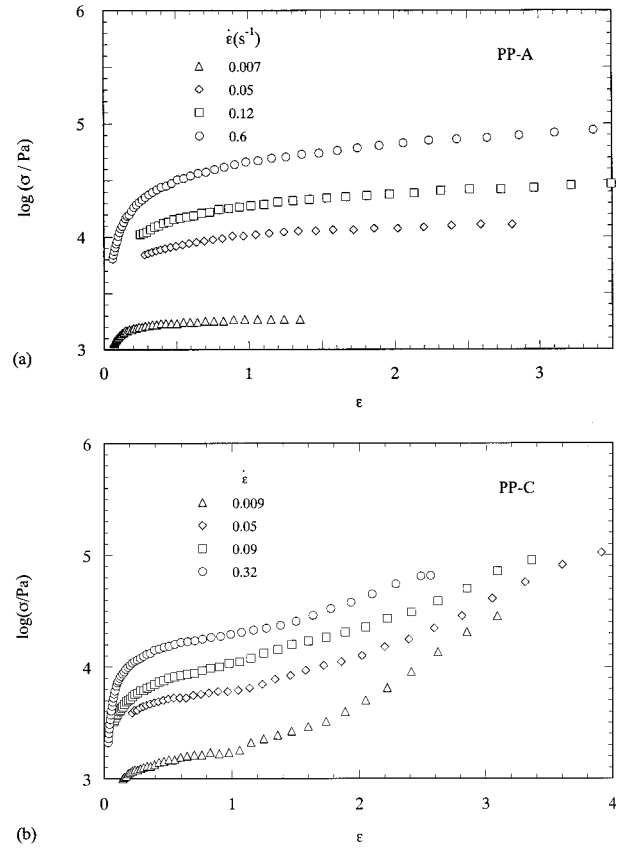

Figure 13. Stress growth as a function of Hencky strain at various strain rates for (a) PP-A and (b) PP-C.

independent of strain rates ($\epsilon \geq 4$). In this region, we may say that the stress growth is predominantly governed merely by the strain, because of extremely long relaxation time of the H-chain. Figure 13a,b indicates stress growth against ϵ for PP-A and PP-C containing uhmw-PE. In Figure 13b, the extensional stress curves at various rates tend to converge at large strain. This behavior would correspond to that of the result of Figure 12 ($\epsilon \geq 4$). Off course, this behavior is not observed for conventional PP which uhmw-PE is not introduced (see Figure 13a). From the above-mentioned, the eminent extensional behavior of PP containing uhmw-PE at large strain may result from the stretch of the uhmw-PE chain.

Concluding Remarks

Our study demonstrates that the high-melt-strength PP (PP-B and PP-C) containing small amounts of PE with high molecular mass show outstanding extensional behavior, that is, strain hardening under uniaxial and biaxial extensional flows. The more intensive strain hardening was observed at lower strain rates. On the other hand, PP-A showed no strain hardening despite the broad molecular weight distribution. The domains observed in the high-melt-strength PP kept the shape before and after extensional deformation. The extensional behavior of a polymer with small amounts of uhmw-chain was estimated by a model proposed by Osaki et al. The model could qualitatively reproduced the stress growth under extensional flow of the binary polymer. The result gave interesting predictions for the extensional viscosity. In part 1, the short and long relaxation time modes were clearly observed for PP-B and PP-C under the shear flow. This long relaxation time mode was revealed also for the fraction which the domains were eliminated by TREF. The extensional flow measurement is very sensitive to the long relaxation time mode and is an available method to judge the miscibility (or immiscibility) of heterogeneous polymer systems. From the facts we have mentioned, we suppose for the high-melt-strength PP that the experimental and theoretical studies in parts 1 and 2 suggest a presence of the effective PE chains dissolved microscopically into PP, leading to the strain hardening under extensional flow.

This study shows the effectiveness and its important role of a long relaxation time mode in order to enhance melt properties of PP. An introduction of long chain may be the exceptional methodology to obtain excellent melt properties without any disadvantages such as decompositions, aggravation of physical properties, etc. The PP with enhanced melt properties will find applications such as foaming, blow molding, thermoforming, and so on. The points made so far about an introduction of a small amounts of uhmw-polymer could apply in principle to any polymer. Recently, considerable progress has been made in polymer dynamics and precision polymerization. This study would be also expected as a guiding principle in designing new materials with desirable processability.

Acknowledgment. The authors thank Dr. G. Marrucci and Dr. D. W. Mead for valuable discussions on the subject matter.

References and Notes

(1) Meissner, J. *Pure Appl. Chem.* **1975**, *42*, 553.
(2) Winter, H. H. *Pure Appl. Chem.* **1983**, *55*, 943.
(3) Schlund, B.; Utracki, L. A. *Polym. Eng. Sci.* **1987**, *27*, 380.
(4) Munstedt, H.; Laun, H. *Rheol. Acta* **1981**, *20*, 211.
(5) Koyama, K.; Ishizuka, O. *Polym. Process Eng.* **1983**, *1*, 55.
(6) Münstedt, H. *J. Rheol.* **1980**, *24*, 847.
(7) Koyama, K.; Ishizuka, O. *J. Soc. Rheol., Jpn.* **1985**, *13*, 93.
(8) Chatraei, S. H.; Macosko, C. W.; Winter, H. H. *J. Rheol.* **1981**, *25*, 433.
(9) Soskey, P. R.; Winter, H. H. *J. Rheol.* **1985**, *29*, 493.
(10) Khan, S. A.; Prud'homme, R. K.; Larson, R. G. *Rheol. Acta* **1987**, *26*, 144.
(11) Nishioka, A.; Takahashi, T.; Masubuchi, Y.; Takimoto, J.; Koyama, K. *J. Non-Newtonian Fluid Mech.* **2000**, *89*, 287.
(12) Takahashi, M.; Isaki, T.; Takigawa, T.; Masuda, T. *J. Rheol.* **1993**, *37*, 827.
(13) Sugimoto, M.; Masubuchi, Y.; Takimoto, J.; Koyama, K. *J. Appl. Polym. Sci.* **1999**, *73*, 1493.
(14) Kurzbeck, S.; Oster, F.; Münstedt, H. *J. Rheol.* **1999**, *43*, 359.

(15) Koyama, K.; Takahashi, T.; Naka, T.; Takimoto, J. Presented at the 13th International Annual Meeting, Polymer Processing Society, Hoboken, NJ, 1997.
(16) Minegishi, A.; Naka, Y.; Takahashi, T.; Masubuchi, Y.; Takimoto, J.; Koyama, K. *J. Soc. Rheol., Jpn.* **1997**, *25*, 215.
(17) Minegishi, A.; Nishioka, A.; Takahashi, T.; Masubuchi, Y.; Takimoto, J.; Koyama, K. Presented at the 14th International Annual Meeting, Polymer Processing Society, Yokohama, Japan, 1998.
(18) Masubuchi, Y.; Takimoto, J.; Koyama, K. *Mol. Simul.* **1999**, *21*, 257.
(19) Meissner, J. *Rheol. Acta* **1969**, *8*, 78.
(20) Papanastasiou, A. C.; Macosko, C. W.; Scriven, L. E. *J. Numer. Methods Fluids* **1986**, *6*, 819.
(21) Nishioka, A.; Takagi, Y.; Takahashi, T.; Masubuchi, Y.; Takimoto, J.; Koyama, K. *J. Soc. Mater. Sci., Jpn.* **1998**, *47*, 1296.
(22) Trouton, F. T. *Proc. R. Soc. London* **1906**, *A77*, 426.
(23) Demarmels, A.; Meissner, J. *Colloid Polym. Sci.* **1986**, *264*, 829.
(24) Laun, H. M.; Schuch, H. *J. Rheol.* **1989**, *33*, 119.
(25) Ebrahimi, N. G.; Takahashi, M.; Araki, O.; Masuda, T. *Acta Polym.* **1995**, *46*, 267.
(26) Ishizuka, O.; Koyama, K. *Polymer* **1980**, *21*, 164.
(27) Higmann, R.; Marczinke, B. L. *J. Rheol.* **1994**, *38*, 573.
(28) Meissner, J.; Stephenson, S. E.; Demarmels, A.; Portmann, P. *J. Non-Newtonian Fluid Mech.* **1982**, *11*, 221.
(29) Urakawa, O.; Takahashi, M.; Masuda, T.; Ebrahimi, N. G. *Macromolecules* **1995**, *28*, 7196.
(30) Padden, J. F. J.; Keith, H. D. *J. Appl. Phys.* **1966**, *37*, 4013.
(31) Bassett, D. C.; Olley, R. H. *Polymer* **1984**, *25*, 935.
(32) Sano, H.; Usami, T.; Nakagawa, H. *Polymer* **1986**, *27*, 1497.
(33) Doi, M.; Edwards, S. F. *The Theory of Polymer Dynamics*; Oxford University: Oxford, 1986.
(34) Münstedt, H.; Kurzbeck, S. *Rheol. Acta* **1998**, *37*, 21.
(35) Tanaka, H.; White, J. *Polym. Eng. Sci.* **1980**, *20*, 949.
(36) Matsumoto, T. *J. Soc. Rheol., Jpn.* **1985**, *13*, 167.
(37) Shikata, T.; Pearson, D. S. *J. Rheol.* **1994**, *38*, 601.
(38) Takahashi, T.; Takimoto, J.; Koyama, K. *Polym. Compos.* **1999**, *20*, 357.
(39) Takahashi, T.; Wu, W.; Toda, H.; Takimoto, J.; Akatsuka, T.; Koyama, K. *J. Non-Newtonian Fluid Mech.* **1997**, *68*, 259.
(40) Marrucci, G. *J. Non-Newtonian Fluid Mech.* **1996**, *62*, 279.
(41) Marrucci, G.; Ianniruberto, G. *Macromol. Symp.* **1997**, *117*, 233.
(42) Sano, H.; Yiu, H.; Hongguo, Li.; Inoue, T. *Polymer* **1998**, *39*, 5265.
(43) Chiang, R. *J. Polym. Sci.* **1959**, *36*, 91.
(44) Osaki, K.; Watanabe, H.; Inoue, T. *J. Soc. Rheol., Jpn.* **1999**, *27*, 63.
(45) McLeish, T. C. B.; Larson, R. G. *J. Rheol.* **1998**, *42*, 81.
(46) Eckstein, A.; Suhm, J.; Friedrich, C.; Maier, R.-D.; Sassmannshausen, J.; Bochmann, M.; Mulhaupt, R. *Macromolecules* **1998**, *31*, 1335.

MA0015525